Biosensors and Bioelectronics 242 (2023) 115743

Contents lists available at ScienceDirect

Biosensors and Bioelectronics

journal homepage: www.elsevier.com/locate/bios

Nanophotonic and hydrogel-based diagnostic system for the monitoring of chronic wounds

Shrishty Bakshi [a,*], Pankaj K. Sahoo [a], Kezheng Li [a], Steven Johnson [a,b], Michael J. Raxworthy [c], Thomas F. Krauss [a,b]

[a] School of Physics, Engineering and Technology, University of York, York, YO10 5DD, UK
[b] York Biomedical Research Institute, University of York, York, YO10 5DD, UK
[c] Neotherix Ltd, Hiscox Building, Peasholme Green, York, YO1 7PR, UK

ARTICLE INFO

Keywords:
Nanophotonics
Chronic wounds
Hydrogel dressing
Wound biomarkers
Non-invasive wound monitoring
Guided mode resonance
Interleukin-6 and Tumor necrosis factor-α

ABSTRACT

Chronic wounds present a major healthcare burden, yet most wounds are only assessed superficially, and treatment is rarely based on the analysis of wound biomarkers. This lack of analysis is based on the fact that sampling of wound biomarkers is typically invasive, leading to a disruption of the wound bed while biomarker detection and quantification is performed in a remote laboratory, away from the point of care. Here, we introduce the diagnostic element of a novel theranostic system that can non-invasively sample biomarkers without disrupting the wound and that can perform biomarker quantification at the point of care, on a short timescale. The system is based on a thermally switchable hydrogel scaffold that enhances wound healing through regeneration of the wound tissue and allows the extraction of wound biomarkers non-destructively. We demonstrate the detection of two major biomarkers of wound health, i.e., IL-6 and TNF-α, in human matrix absorbed into the hydrogel dressing. Quantification of the biomarkers directly in the hydrogel is achieved using a chirped guided mode resonant biosensor and we demonstrate biomarker detection within the clinically relevant range of pg/mL to μg/mL concentrations. We also demonstrate the detection of IL-6 and TNF-α at concentration 1 ng/mL in hydrogel dressing absorbed with clinical wound exudate samples. The high sensitivity and the wide dynamic range we demonstrate are both essential for the clinical relevance of our system. Our test makes a major contribution towards the development of a wound theranostic for guided treatment and management of chronic wounds.

1. Introduction

Chronic wounds are defined as wounds that do not heal in an orderly or timely manner or that take excessive time to heal (Kyaw et al., 2018). These wounds are a matter of major concern, because they not only cause severe distress to afflicted patients, but also present a major burden to healthcare systems with associated comorbidities (Ochoa et al., 2014). In the UK alone, the management of chronic wounds was estimated to cost the NHS £5.3 bn per year, around 4 percent of the total NHS budget (Guest et al., 2017). Similarly, in the US, chronic wounds affect 5.7 million people at an annual cost of $20 bn (Jarbrink et al., 2017). These statistics highlight the need for better approaches to assess wound health and inform appropriate and timely treatment and management.

The progression of wounds through haemostasis, inflammation, proliferation and remodeling (Ochoa et al., 2014) is tightly governed by the presence and actions of systemic proteins (such as cytokines, growth factors and enzymes) and by the local microbiome (Wilkinson and Hardman., 2020). Wounds have traditionally been managed with debridement and different types of topical treatments and dressings (Han and Ceilley., 2017). The idea of using a regenerative polymeric scaffold (Negut et al., 2020) with the option for this to contain antimicrobial agents (Contreras et al., 2019) has developed more recently, as has the concept of integrating diagnostic sensors to complement and inform wound management (Tang et al., 2021). Such platforms, ideally combining therapy and diagnostics ("theranostics") offer the simultaneous benefit of an improved understanding of non-healing wounds alongside improved treatment, leading to reduced hospitalisation times (Dargaville et al., 2013; Eriksson et al., 2022).

Wound dressings based on hydrogels have been developed for some

* Corresponding author.
E-mail address: shrishty.bakshi@york.ac.uk (S. Bakshi).

https://doi.org/10.1016/j.bios.2023.115743
Received 19 June 2023; Received in revised form 2 October 2023; Accepted 5 October 2023
Available online 6 October 2023

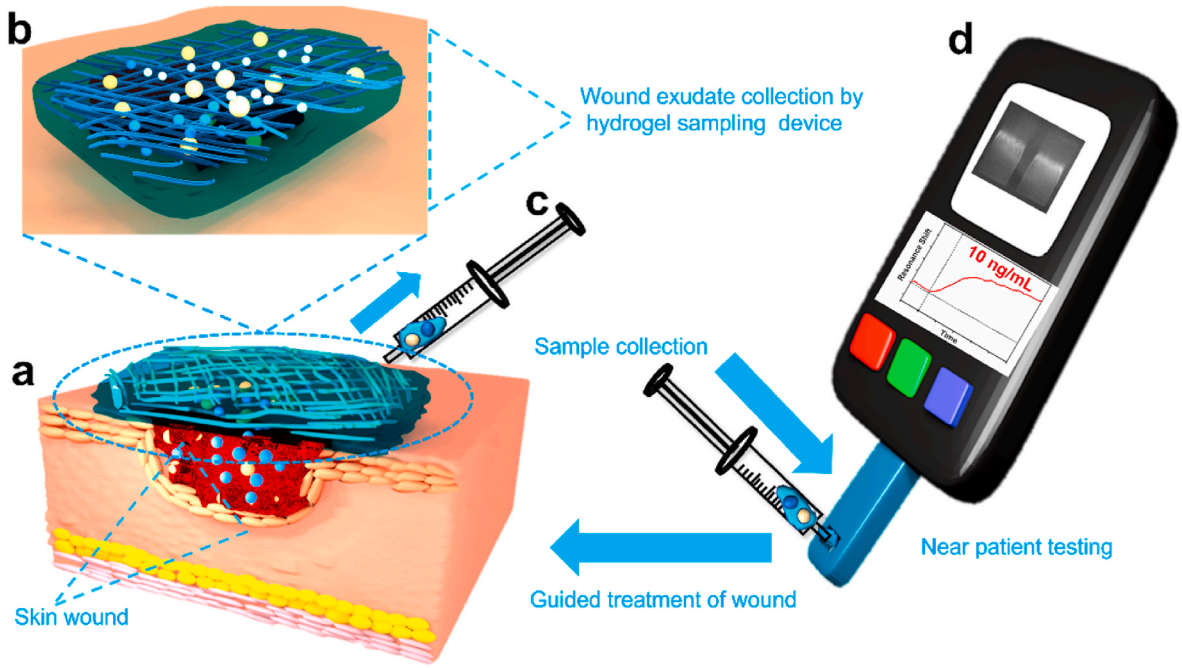

Fig. 1. Schematic of the proposed diganostic system for monitoring chronic wounds. The hydrogel based dressing enables non-destructive sampling of the wound exudate for analysis to inform treatment. (a) Hydrogel wound dressing based sampling device placed on skin wound. (b) Magnified image showing wound fluid absorbed in hydrogel based dressing placed on skin wound. (c) Wound fluid absorbed dressing collection from skin wound. (d) Near patient testing device to detect wound biomarkers in wound fluid absorbed dressing.

time, as they can be loaded with therapeutic agents to support and manage wound healing (Liang et al., 2021; Tavakoli and Klar., 2020). In addition, the hydrogel can be formulated to allow for the extraction of the wound exudate or for the micro-sampling of material released into the wound space without disrupting the wound [https://www.neotherix.com, US 10,687,790]. The key for this non-disruptive sampling is the thermally controlled viscosity of the gel, which has low viscosity at low temperature, allowing extraction, while it has high viscosity at body temperature, enabling the formation of a solid gel-based dressing. The challenge we address here is to demonstrate the detection and quantification of biomarkers relevant to the progression and trajectory of wound healing at clinically relevant levels in this hydrogel matrix.

1.1. Importance of measuring biomarkers to measure the wound healing trajectory

Cytokines and proteases are the most useful biomarkers for monitoring the wound-healing process. Studies have found raised levels of biomarkers such as MMP, the MMP/TIMP ratio, cytokines, procalcitonin, and myeloperoxidase in non-healing wounds (Yussof et al., 2012). Similarly, the levels of TNF-α and IL-6 levels have been observed to be elevated in non-healing wounds. For example, Trengove et al. showed that the levels of TNF-α and IL-6 were in the range of 1 ng/mL - 13 ng/mL and 28 ng/mL −210 ng/mL for non-healing wounds respectively as decribed in table S8 (Trengove et al., 2000), although there is a significant variation between patients. The identification of biomarkers indicative of wound healing is therefore an on-going research topic, but it is already clear that the detection of multiple biomarkers is essential for an accurate diagnosis and that TNF-α and IL-6 have an important role to play; we therefore focus on the detection of these two markers.

Currently, the levels of these biomarkers are determined using laboratory techniques, such as enzyme-linked immunoassay (ELISA) (Nimse et al., 2016), chemiluminescence (Li et al., 2018) and immuno-PCR (M Komatsu et.al., 2001). Conducting such tests at the bedside would be very desirable in order to reduce the time to result. Unfortunately, the products currently available on the market only address this need to a limited extent. For example, Woundchek (https://www.woundchek.com), has limited sensitivity and only measures a single marker; MolecuLight (https://moleculight.com/) only samples bacteria using autofluorescence. Other modalities include electrochemical voltammetry (Liu et al., 2012; Weng et al., 2013), electrochemical impedance (Kongsuphol et al., 2014; Pui et al., 2013) and calorimetric sensor (Xin Ting Zheng et al., 2023a; Zheng et al., 2023b). A table comparing different types of sensors developed for wound monitoring is provided in supplementary information table S9. Some of these have not yet demonstrated sufficient sensitivity and do not yet offer the ease of use required for use by non-specialists. Recently, Gao et al. reported a flexible electrochemical wound biomarker sensor (Yuji Gao et al., 2021), but their approach was not integrated into a theranostic and electrochemical sensors are known to suffer from long-term drift (Laref et al., 2021; Lin et al., 2020; Popoola et al., 2016), which is an issue when monitoring biomarker levels over extended periods with low-cost portable instrumentation. In brief, the long term continuous monitoring of chronic wounds is still a major challenge (Lu et al., 2022).

Here, we demonstrate the chirped, guided mode resonance (GMR) sensor modality for the monitoring of chronic wound biomarkers. GMR sensors use optical transduction to enable contact-free and label-free detection of biomarkers and have already demonstrated ELISA-level performance (pg/mL) in a clinical matrix (Kenaan et al., 2020). We have also demonstrated the multiplexing capability of this approach, by showing the parallel detection of up to 4 different biomarkers (Kenaan et al., 2020), which is highly relevant to the wound monitoring problem. The grating sensors operate by coupling collimated light into a high refractive index silicon nitride grating. This process sets up a leaky standing wave, termed the guided mode resonance (GMR) which forms an evanescent wave tail outside the grating thus making it sensitive to external refractive index changes. On resonance, the light is reflected back, which is detected. By varying the period of the grating, the position of the backreflected light varies in position, so the chirped grating maps spectral information onto spatial information, which is easily detected by imaging the grating onto a camera. We have already shown that such a GMR sensor can be realised as a handheld instrument

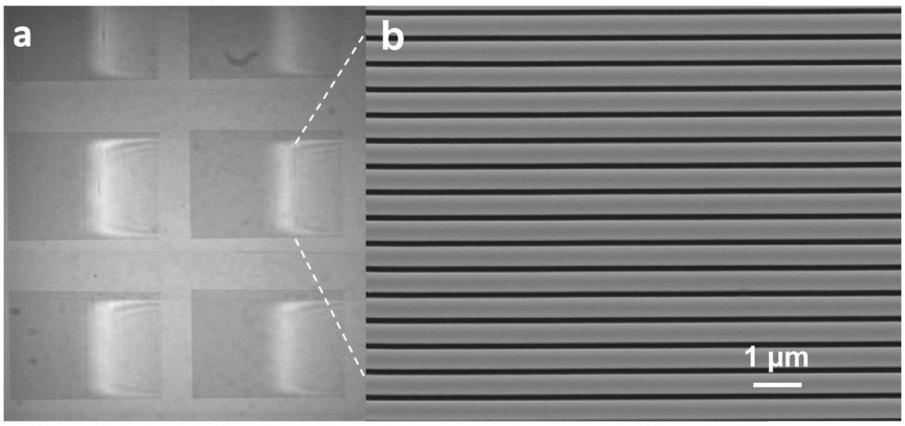

Fig. 2. a) Optical micrograph of the resonance on the chirped GMR grating, taken in reflection. The vertical light bar shows the resonance observed in reflection from a typical chirped GMR. (b) scanning electron micrograph of the grating. The period is varied between 432 and 440 nm and the filling factor is 0.7. The gratings are designed for a resonance wavelength around 650 nm.

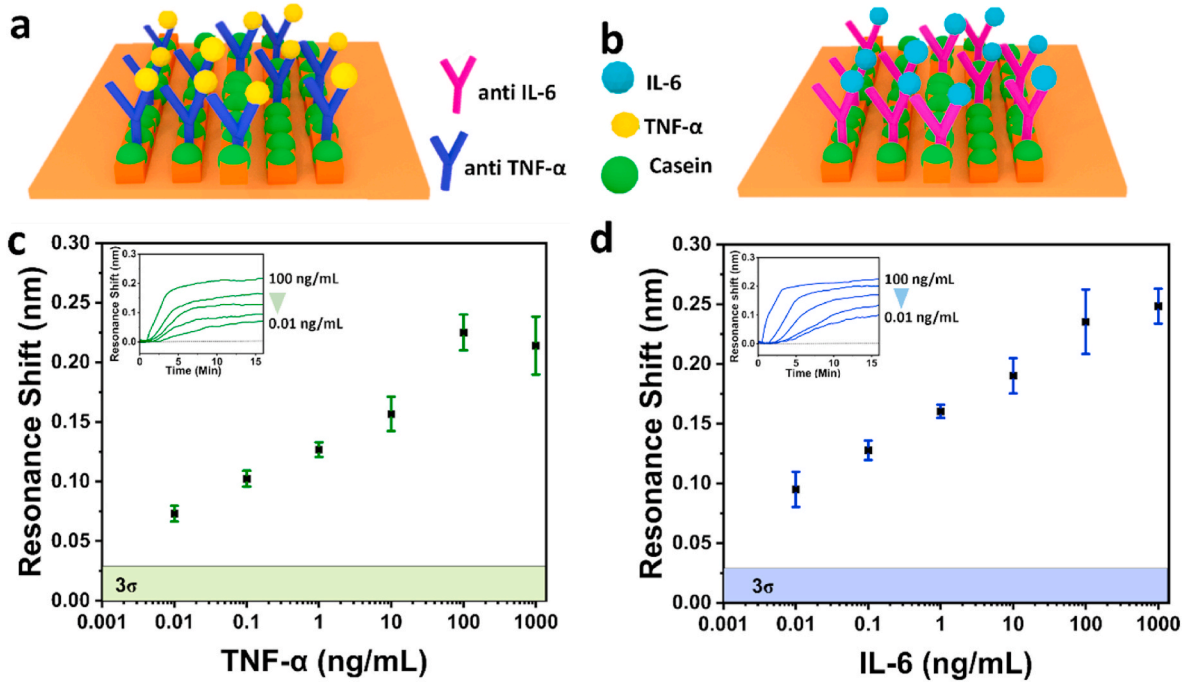

Fig. 3. Surface chemistry and characterisation of the GMR biosensor for TNF-α and IL-6 detection. (a and b) Polydopamine surface chemistry was used for the anti-TNF-α and anti-IL-6 immobilisation on GMR sensors, followed by the blocking of remaining sites with casein in order to observe selective binding and to minimise fouling. (c) Resonance shifts observed for TNF-α concentrations ranging from 0.01 ng/mL to 1 μg/mL. The inset shows the binding curves for the same. (d) Resonance shift for IL-6 protein in PBS buffer at concentrations ranging from 0.01 ng/mL to 1 μg/mL. The binding curves for the same are shown in the inset. The error bars correspond to the standard deviation for three separate experiments for each concentration.

manufactured using low-cost components (Drayton et al., 2020). We now show that this device is also well suited for monitoring the wound healing process as a near-patient test, by measuring key biomarkers in a hydrogel-based wound dressing system. The test can be used to monitor biomarkers in wound exudate in a non-invasive and repeated manner Fig. 1.

2. Materials and methods (See supplementary information S1–S5)

2.1. GMR sensors

The grating sensors were fabricated using electron beam lithography and were designed to exhibit a resonance in at 650 nm. The range of the resonance is 10 nm in wavelength, from 642 nm to 652 nm which corresponds to the period change from 432 to 440 nm with a filling factor of 0.7. This wavelength was chosen for technological reasons, such as the compatibility with CMOS cameras, high performance of silicon nitride as the optical material and the availability of low-cost, high brightness sources such as 650 nm resonant cavity LEDs. The vertical line constituting the optical resonance is shown in Fig. 2a and a scanning electron micrograph of the sensor is shown in Fig. 2b.We have already shown (Drayton et al., 2020) that the same quality sensor can be produced by nanoimprint lithography, making manufacture compatible with our low-cost vision.

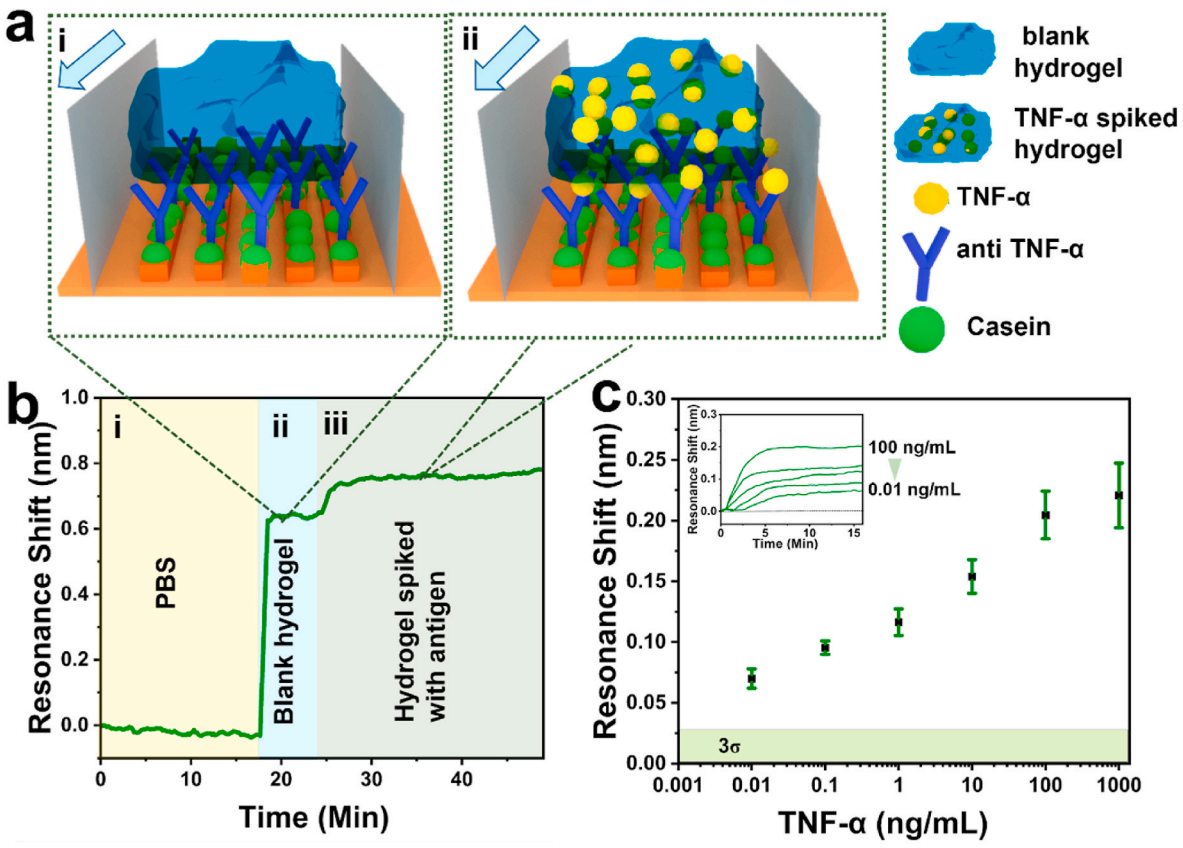

Fig. 4. a) Schematic of the experiment, illustrating that blank hydrogel is introduced first, followed by spiked hydrogel. The arrows representing the direction of flow of sample in microfluidic channel. b) Biorecognition assay performed in hydrogel. Firstly, blank hydrogel (ii) is introduced into the channel to quantify the resonance shift caused by the refractive index of the hydrogel solution. This is followed by introducing hydrogel spiked with antigen (iii) to obtain the shift caused by the antibody-antigen binding. (c) Resonance shifts observed for TNF-α of concentrations ranging from 0.01 ng/mL to 1 μg/mL. The inset shows the binding curves for different concentrations. The error bars correspond to the standard deviation derived from three separate experiments for each concentration.

3. Results and discussion

3.1. Detection of TNF-α and IL-6 in PBS buffer

A robust and stable surface chemistry is critical for affinity-based biosensors to ensure sensitive, selective and reliable immunodetection of the analytes of interest from a complex matrix. Here, we coated the GMR sensor surface with a polydopamine film of a few nanometres thickness to immobilise the antibodies. This was followed by applying casein to block the remaining binding sites and to reduce nonspecific binding. To characterise the surface chemistry, following the surface functionalisation protocol described in S5.1 and S5.2, we exposed the sensors to TNF-α and IL-6 with different concentrations ranging from 0.01 ng/mL to 1 μg/mL. The shift of the resonance position is shown in Fig. 3c and d while the relevant insets show binding curves for the various concentrations. The shifts observed for the lowest concentration of 0.01 ng/mL of TNF-α, and IL-6 are ~0.07 nm and ~0.09 nm, respectively, both of which are above the 3σ value of the system which is 0.028 nm ± 0.003 (n = 10).

3.2. Wound biomarker detection in hydrogel

Next, we conducted the same experiment as in PBS but with hydrogel as the matrix (Fig. 4). The key questions are a) whether the long polymeric chains associated with the hydrogel would interfere with the formation of the antibody-antigen complex and b) whether the bulk RI change associated with the hydrogel would dominate the GMR response and mask detection of antigen binding. In order to identify the impact of these effects, we conducted the following assay. After performing the biofunctionalisation, i.e., the steps described in S5.1 and S5.2 (full assay fig S6), we first introduced hydrogel into the channel to quantify the shift in resonance due to the refractive index change caused by the hydrogel solution (Fig. 4ai and 4bii). This was followed by the same hydrogel spiked with antigen (Fig. 4a ii and 4b iii) in order to understand if the hydrogel interfered with the binding between antigen and antibody. After subtracting the effect of the refractive index change induced by the hydrogel, the binding curve saturated for a resonance shift of $\Delta\lambda \approx 0.2–0.25$ nm, irrespective of the presence of the hydrogel, i.e. the resonance shift is comparable for both TNF-α assays (compare Fig. 3c and 4c) within experimental error; this confirms that the hydrogel does not interfere with binding and that the refractive index shift it causes can be simply subtracted. Overall, this shows that our biosensing interface designed is sufficiently robust to perform measurements in hydrogel.

3.3. Biomarker detection in human matrix

As the final, and most important experiment, we exposed the sensors to human matrix absorbed by the hydrogel dressing as described in S4. The human matrix consists of a mixture of human plasma and human serum, which is physiologically identical to wound exudate (Spear., 2012). The matrix was spiked with TNF-α and IL-6. We used a reference channel to account for any fouling effect; specifically, to separate the shift arising from specific binding from that due to non-specific binding, we used a reference channel that was blocked with casein only and that did not contain antibodies, such that it would still be sensitive to changes in bulk RI and non-specific binding, but not to the RI change associated with specific antibody-antigen binding (fig: S7). The

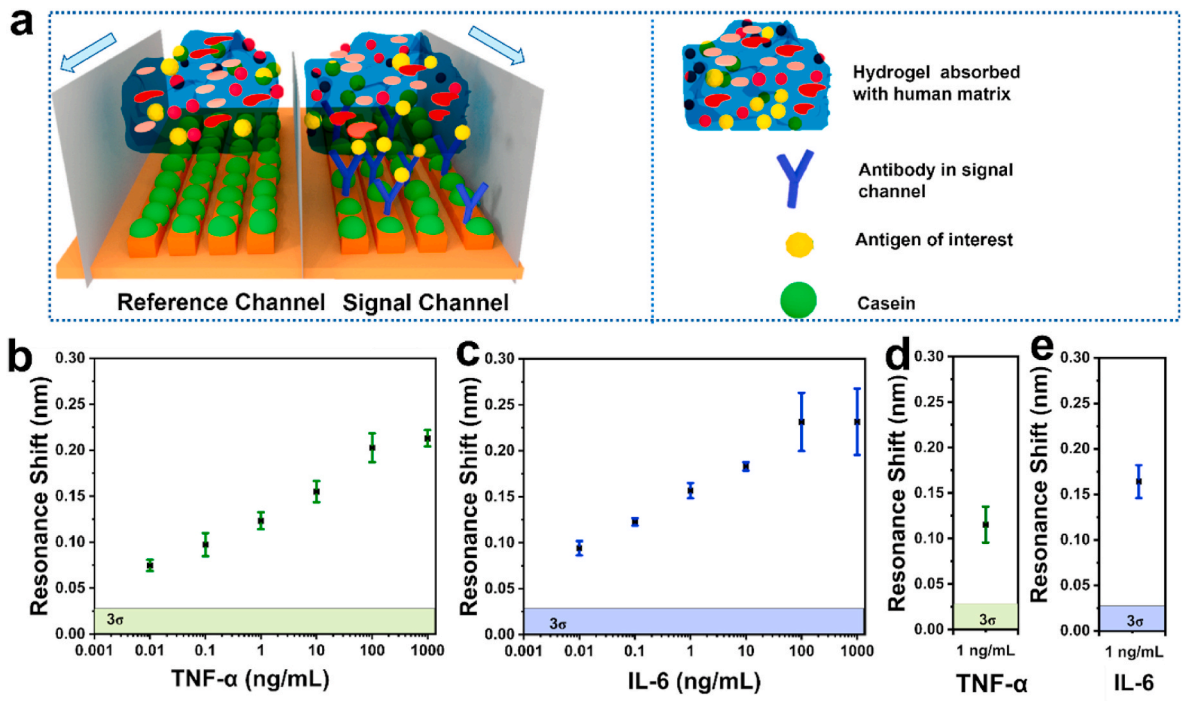

Fig. 5. (a) Schematic of the biorecognition assay used to detect TNF-α and IL-6 on both the signal and the reference channels. The arrow in Fig. 5a represents the direction of flow of sample in microfluidic channel. b) and c) Differential resonance shifts obtained by subtracting the shift observed in reference channel from the shift observed in signal channel for TNF-α and IL-6 binding, spiked into human matrix absorbed dressings for concentrations varying from 0.01 ng/mL to 1 μg/mL (d) and (e) Resonance shifts observed for the 1 ng/mL TNF-α and IL-6 spiked in the hydrogel dressing absorbed with clinical wound exudate acquired from the hospital. The error bars correspond to the standard deviation derived from three separate experiments for each concentration.

corresponding wavelength shifts are shown in Fig. 5b and c. Critically, the resonance shifts observed in Figs. 3 and 5 are comparable, indicating the robustness of the system and its ability to perform measurements in complex human matrices absorbed in hydrogel based dressings. In addition to that we have performed measurement in clinical wound exudate absorbed dressing acquired from the hospital. The clinical wound exudate absorbed dressing was spiked with 1 ng/mL of IL-6 and TNF-α as the clinically relevant concentrations of both of these biomarkers in healing and non -healing wounds are above this value as described in table S8. The resonance shifts observed for the detection of 1 ng/mL of TNF-α and IL-6 spiked in clinical wound exudate absorbed hydrogel dressing Fig 5d and e are similar to that observed in human matrix Fig. 5b and c and phosphate buffer saline Fig. 3c and d. These results indicate the suitability of developed biosensing system for the clinical patient samples.

4. Conclusion

We report progress towards the development of a nanophotonic theranostic system for the non-invasive monitoring and improved management of chronic wounds. We demonstrate the successful detection of two important wound biomarkers, i.e., TNF-α and IL-6 in a clinically relevant matrix. Remarkably, we observe very similar resonance shifts for antigens spiked into phosphate buffer saline (PBS), hydrogel and human matrix absorbed hydrogel dressings. We have also studied the applicability of this system with clinical wound sample acquired from the hospital and observed the similar resonance shifts for 1 ng/mL of TNF-α and IL-6 as we in the other above mentioned matrix. This similarity highlights the high quality and the robustness of the biosensing interface we have developed. Both the sensitivity and the dynamic range are essential for the clinical relevance of the theranostic to account for variations between patients and for assessing different stages of wound healing. As an important next step, our test needs to be expanded to monitor other relevant biomarkers, such as MMP-9 and protease enzymes, using the multiplexing capability we have already demonstrated (Kenaan et al., 2020). Furthermore, a larger scale patient study is required for a better understanding of the correlation between biomarker concentration and the wound healing process, and to inform the clinically actionable outcome. With these future improvements, we believe that our approach can be used with a wide range of hydrogel-based wound dressings and form the basis of a low-cost near patient theranostic would healing system.

CRediT authorship contribution statement

Thomas F. Krauss and Michael J. Raxworthy conceived the experiments and decided on the use of biomarkers. Shrishty Bakshi designed and conducted the experiments. Shrishty Bakshi performed the data analysis (together with Kezheng Li). Pankaj K. Sahoo and Kezheng Li fabricated the guided mode resonance sensor chips used in the study. Data was interpreted by Steven Johnson, Thomas F. Krauss and Shrishty Bakshi. Shrishty Bakshi and Thomas F. Krauss wrote the paper with comments by all authors.

Declaration of competing interest

The authors declare that they have no known competing financial interests or personal relationships that could have appeared to influence the work reported in this paper.

Data availability

Data will be made available on request.

Acknowledgements

We gratefully acknowledge support by the EPSRC of the UK (Grant numbers EP/V047434/1 and EP/R51181X/1). We would also like to

acknowledge Professor Matthew J. Hardman, Wound Group Lead – Biomedical Institute of Multimorbidity, Hull-York Medical School, for providing clinical wound exudate.

Appendix A. Supplementary data

Supplementary data to this article can be found online at https://doi.org/10.1016/j.bios.2023.115743.

References

Contreras, A., Raxworthy, M.J., Wood, S., Schiffman, J.D., Tronci, G., 2019. Photodynamically active electrospun fibers for antibiotic-free infection control. ACS Appl. Bio Mater. 2 (10), 4258–4270.

Dargaville, T.R., Farrugia, B.L., Broadbent, J.A., Pace, S., Upton, Z., Voelcker, N.H., 2013. Sensors and imaging for wound healing: a review. Biosens. Bioelectron. 41, 30–42.

Drayton, A., Li, K., Simmons, M., Reardon, C., Krauss, T.F., 2020. Performance limitations of resonant refractive index sensors with low-cost components. Opt Express 28 (22), 32239–32248.

Eriksson, E., Liu, P.Y., Schultz, G.S., Martins-Green, M.M., Tanaka, R., Weir, D., Gould, L. J., Armstrong, D.G., Gibbons, G.W., Wolcott, R., Olutoye, O.O., Kirsner, R.S., Gurtner, G.C., 2022. Chronic wounds: treatment consensus. Wound Repair Regen. 30 (2), 156–171.

Gao, Yuji, Nguyen, Dat T., Yeo, Trifanny, Lim, Su Bin, Tan, Wei Xian, Madden, Leigh Edward, Jin, Lin, Kenan Long, Ji Yong, Abu Bakar Aloweni, Fazila, Angela Liew, Yi Jia, Li Ling Tan, Mandy, Yuh Ang, Shin, D/O Maniya, Sivagame, Abdelwahab, Ibrahim, Ping Loh, Kian, Chen, Chia-Hung, Laurence Becker, David, Leavesley, David, Ho, John S., Lim, C.T., 2021. A flexible multiplexed immunosensor for point-of-care in situ wound monitoring. Sci. Adv. 7 (21), 1–15.

Guest, J.F., Ayoub, N., McIlwraith, T., Uchegbu, I., Gerrish, A., Weidlich, D., Vowden, K., Vowden, P., 2017. Health economic burden that different wound types impose on the UK's National Health Service. Int. Wound J. 14 (2), 322–330.

Han, G., Ceilley, R., 2017. Chronic wound healing: a review of current management and treatments. Adv. Ther. 34 (3), 599–610.

Jarbrink, K., Ni, G., Sonnergren, H., Schmidtchen, A., Pang, C., Bajpai, R., Car, J., 2017. The humanistic and economic burden of chronic wounds: a protocol for a systematic review. Syst. Rev. 6 (1), 15.

Kenaan, A., Li, K., Barth, I., Johnson, S., Song, J., Krauss, T.F., 2020. Guided mode resonance sensor for the parallel detection of multiple protein biomarkers in human urine with high sensitivity. Biosens. Bioelectron. 153, 112047.

Komatsu, D.K., Saito, K., Furuya, D., Yagihashi, A., Araake, H., Tsuji, N., Sakamaki, S., Niitsu, Y., Watanabe, N., 2001. Tumor necrosis factor-alpha in serum of patients with inflammatory bowel disease as measured by a highly sensitive immuno-PCR. Clin. Chem. 47 (7), 1297–1301.

Kongsuphol, P., Ng, H.H., Pursey, J.P., Arya, S.K., Wong, C.C., Stulz, E., Park, M.K., 2014. EIS-based biosensor for ultra-sensitive detection of TNF-alpha from non-diluted human serum. Biosens. Bioelectron. 61, 274–279.

Kyaw, B.M., Jarbrink, K., Martinengo, L., Car, J., Harding, K., Schmidtchen, A., 2018. Need for improved definition of "chronic wounds" in clinical studies. Acta Derm. Venereol. 98 (1), 157–158.

Laref, R., Losson, E., Sava, A., Siadat, M., 2021. Empiric unsupervised drifts correction method of electrochemical sensors for in field nitrogen dioxide monitoring. Sensors 21 (11), 3581.

Li, G., Wu, W., Zhang, X., Huang, Y., Wen, Y., Li, X., Gao, R., 2018. Serum levels of tumor necrosis factor alpha in patients with IgA nephropathy are closely associated with disease severity. BMC Nephrol. 19, 326.

Liang, Y., He, J., Guo, B., 2021. Functional hydrogels as wound dressing to enhance wound healing. ACS Nano 15 (8), 12687–12722.

Lin, J., Gao, H., Wang, X., Yang, C., Xin, Y., Zhou, X., 2020. Effect of temperature on the performance of electrochemical seismic sensor and the compensation method. Measurement 155, 107518.

Liu, Y., Kwa, T., Revzin, A., 2012. Simultaneous detection of cell-secreted TNF-alpha and IFN-gamma using micropatterned aptamer-modified electrodes. Biomaterials 33 (30), 7347–7355.

Lu, S.-H., Samandari, M., Li, C., Li, H., Song, D., Zhang, Y., Tamayol, A., Wang, X., 2022. Multimodal sensing and therapeutic systems for wound healing and management: a review. Sensor Actuators Rep. 4.

Negut, I., Dorcioman, G., Grumezescu, V., 2020. Scaffolds for wound healing applications. Polymers 12 (9), 2010.

Nimse, S.B., Sonawane, M.D., Song, K.S., Kim, T., 2016. Biomarker detection technologies and future directions. Analyst 141 (3), 740–755.

Ochoa, M., Rahimi, R., Ziaie, B., 2014. Flexible sensors for chronic wound management. IEEE Rev. Biomed. Eng. 7, 73–86.

Popoola, O.A.M., Stewart, G.B., Mead, M.I., Jones, R.L., 2016. Development of a baseline-temperature correction methodology for electrochemical sensors and its implications for long-term stability. Atmos. Environ. 147, 330–343.

Pui, T.S., Kongsuphol, P., Arya, S.K., Bansal, T., 2013. Detection of tumor necrosis factor (TNF-α) in cell culture medium with label free electrochemical impedance spectroscopy. Sensor. Actuator. B Chem. 181, 494–500.

Spear, M., 2012. Wound exudate-the good, the bad, and the ugly. Plast. Surg. Nurs. 32 (2), 77–79.

Tang, N., Zheng, Y., Cui, D., Haick, H., 2021. Multifunctional dressing for wound diagnosis and rehabilitation. Adv. Healthcare Mater. 10 (22), e2101292.

Tavakoli, S., Klar, A.S., 2020. Advanced hydrogels as wound dressings. Biomolecules 10 (8), 1169.

Trengove, N.J., Bielefeldt-Ohmann, H., Stacey, M.C., 2000. Mitogenic activity and cytokine levels in non-healing and healing chronic leg ulcers. Wound Repair Regen. 8 (1), 13–25.

Weng, S., Chen, M., Zhao, C., Liu, A., Lin, L., Liu, Q., Lin, J., Lin, X., 2013. Label-free electrochemical immunosensor based on K3[Fe(CN)6] as signal for facile and sensitive determination of tumor necrosis factor-alpha. Sensor. Actuator. B Chem. 184, 1–7.

Wilkinson, H.N., Hardman, M.J., 2020. Wound healing: cellular mechanisms and pathological outcomes. Open Biol. 10 (9), 200223.

Zheng, Xin Ting, Zijie Yang, L.S., Moogaambikai Thangaveloo, Y.Y., Mohamed Salleh, Nur Asinah Binte, Jiah Shin Chin, Z.X., David Lawrence, Becker, Loh, X.J., Benjamin, C.K., Tee, X.S., 2023. Battery-free and AI-enabled multiplexed sensor patches for wound monitoring. Sci. Adv. 9, 1–16.

Yussof, S.J.M., Omar, E., Pai, D.R., Sood, S., 2012. Cellular events and biomarkers of wound healing. Indian J. Plastic Surg. 45, 220–228.

Zheng, X.T., Zhong, Y., Chu, H.E., Yu, Y., Zhang, Y., Chin, J.S., Becker, D.L., Su, X., Loh, X.J., 2023. Carbon dot-doped hydrogel sensor array for multiplexed colorimetric detection of wound healing. ACS Appl. Mater. Interfaces 15 (14), 17675–17687.